

ADSORPTION OF AuCl_4^- BY KAOLINITES: EFFECT OF pH, TEMPERATURE AND KAOLINITE CRYSTALLINITY

HANLIE HONG^{1,*}, ZHENYA SUN¹, ZHENGYI FU² AND XINMIN MIN²

¹ The Center for Materials Testing and Research, ² National Key Laboratory of Advanced Technology for Materials Synthesis and Processing, Wuhan University of Technology, Wuhan, Hubei 430070, PR China

Abstract—Adsorption of the AuCl_4^- complex by kaolinites of different crystallinities (Kao-1 and Kao-2) from 100 mL of $\text{AuCl}_3\cdot\text{HCl}\cdot4\text{H}_2\text{O}$ solutions containing 10,000, 500 and 50 $\mu\text{g/L}$ Au and 1 g of kaolinite was measured at pH 3 to 9 at ambient temperature and 120°C. Adsorption from the 50, 500 and 10,000 μg Au/L solutions ranged from 64 to 100% at ambient temperature and from 68 to 100% at 120°C for both kaolinites. Adsorption was pH dependent with a maximum at pH <5 and a minimum at neutral and alkaline pHs. Up to 1 mg Au/g kaolinite was adsorbed by the kaolinites at both ambient temperature and 120°C. In a separate Au adsorption experiment using 100 mL of 4000 μg Au/L solutions and 0.02 to 1.0 g of Kao-1, up to 8.55 mg Au/g of kaolinite was adsorbed. The pH dependence of Au adsorption suggests that surface complexation of Au to alumina sites at the edges of kaolinite particles might be involved. Protonation of kaolinite surface sites might facilitate adsorption of the anionic Au complex. Both kaolinites adsorbed ~100% of added Au at low pH values, but the less crystalline kaolinite (Kao-2) adsorbed more Au at high pH. Greater Au adsorption would be expected for the less crystalline Kao-2 sample if adsorption occurred at the edges of kaolinite particles.

Key Words—Adsorption, Crystallinity, Isotherm, Kaolinite, Surface Complexation.

INTRODUCTION

It is generally accepted that Au can be complexed by a comprehensive range of ligands and it is relatively soluble in the supergene environment, depending on the activity of the ligand, the oxidation-reduction potential (Eh) and solution pH. In acidic solutions, chloride is the ligand most capable of complexing Au, mainly as AuCl_4^- (Ogryzlo, 1935), which is extremely stable in hydrothermal fluids over a wide range of pH and temperatures and is believed to be one of the principal ions responsible for leaching and transport of Au (Seward, 1973, 1984; Renders and Seward, 1989).

Previous work has focused predominantly on the role of natural sulfide surfaces in the adsorption/reduction reactions of metals and precious metal complexes based on the intimate relationship between Au and sulfide in the deposits (Hyland and Bancroft, 1989; Mycroft *et al.*, 1995). However, the association of clay minerals with the so-called ‘invisible gold’, which are present as extremely fine particles $<1000 \text{ \AA}$, not detectable by optical or scanning electron microscopy, has also been recognized since this kind of gold deposit was found in the 1970s. Foster (1970) pointed out that most of the Carlin gold is related to clay minerals, kaolinite and hydromica. In the oxidized zone, clay minerals play an important role in Au accumulation during the Au mineralization process (Boyle, 1979). Recently, transmission electron microscopy (TEM) investigation

proved that the so-called ‘invisible gold’ was adsorbed on the edges of clay minerals, kaolinite and illite (Ye *et al.*, 1994; Hong and Ye, 1998; Hong *et al.*, 1999). It was inferred that the Au-bearing complex can be adsorbed onto the surfaces of clay minerals and, therefore, resulted in the accumulation of Au. Rosliyakov (1990) claimed that Au is adsorbed on the crystal surface of clay minerals, though there is an adequately strong adsorption bond between Au and the clay minerals for it to be considered as chemical adsorption.

In this study we report the effect of pH, temperature and kaolinite crystallinity on the adsorption of the AuCl_4^- complex by kaolinites. Our experiments were carried out in three different concentrations of Au: 50, 500 and 10,000 $\mu\text{g/L}$, at ambient temperature and 120°C, respectively. We measured the amount of Au scavenged by kaolinites from solutions of different concentrations. Finally, we investigated the adsorption models of AuCl_4^- complex on kaolinite at ambient temperature and at pH of 5. The objective of this study was to investigate the adsorption of Au from $\text{AuCl}_3\cdot\text{HCl}\cdot4\text{H}_2\text{O}$ solutions by kaolinites at ambient temperature and 120°C and to understand the adsorptive properties of kaolinite for the simple gold chloride complex AuCl_4^- and, hence, to gain a better understanding of the adsorption process by which Au is concentrated in deposits of this kind.

EXPERIMENTAL METHODS

Preparation of the samples

Two kinds of kaolinite samples with different crystallinity were used to evaluate the effect of crystal-

* E-mail address of corresponding author:
honghl@public.wh.hb.cn
DOI: 10.1346/CCMN.2003.0510503

linity on adsorption. The kaolinites were collected from Jiepai, Hunan (Kao-1) and Yangshan, Jiangsu (Kao-2). Both of the kaolinite separates were prepared using the pulverized ore sample and a method of precipitation. For investigation of adsorption models, the Kao-1 sample was further separated using gravity sedimentation techniques. The grain-size was estimated to be $<2\text{ }\mu\text{m}$ from the speed of precipitation.

Mineralogical characteristics of the kaolinites

X-ray diffraction (XRD), scanning electron microscope (SEM) and TEM evidence confirmed that both of the samples, after purification, were of high purity. The XRD patterns were recorded using a Rigaku D/MAX-III A diffractometer using Ni-filtered $\text{CuK}\alpha$ radiation from 2 to $60^\circ 2\theta$ at a scan rate of $2^\circ 2\theta \text{ min}^{-1}$ (Figure 1). The data were used to calculate the Hinckley crystallinity index. The SEM analysis was undertaken on an SX-40 scanning electron microscope at 20 kV accelerating voltage and a beam current in the range 1–3 nA. The particles of Kao-1 appeared larger and thicker than the particles of Kao-2 (Figure 2). Moreover, further observations of the two samples by TEM, performed on an Hitachi 800 transmission electron microscope at 120 kV, indicated that Kao-1 particles tend to have hexagonal outlines and basal-plane steps showing clear crystallographic control, whereas Kao-2 particles have more rounded hexagonal outlines and irregular basal-plane surface microtopography (Figure 3).

Particle-size analysis was made on a Vicom image analyzer (Table 1). The chemical composition of the samples was obtained by a wet chemical method for the main constituents SiO_2 , Al_2O_3 and H_2O^+ , and by plasma atomic emission spectrometer for the secondary constituents Fe_2O_3 , MgO , CaO , Na_2O , K_2O , MnO and TiO_2 , which was done on a PLASMA 300 inductively coupled plasma atomic emission spectrometer (Table 2).

Adsorption of the AuCl_4^- complex

Both of the samples were cleaned prior to adsorption experiments to remove contaminant materials adsorbed on their surfaces according to Sutheimer *et al.* (1999). The cleaning procedure consisted of washing the sample

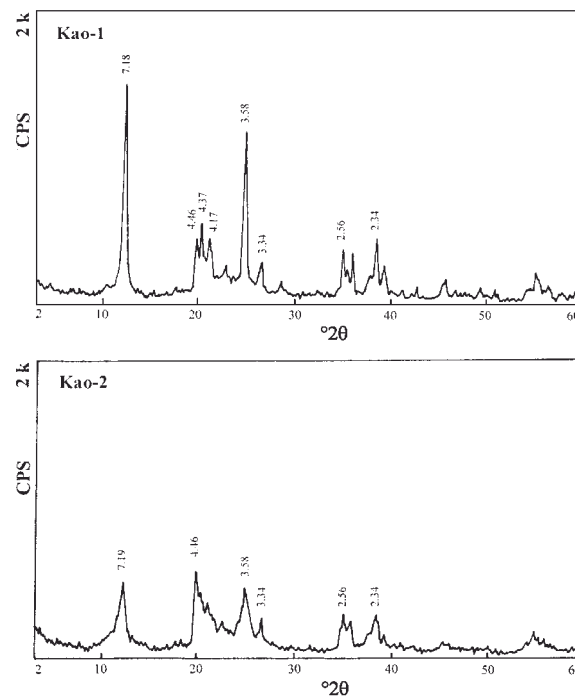


Figure 1. XRD traces showing the purity and crystallinity of the two kaolinites. Kaolinite Kao-1 is well crystallized and Kao-2 is poorly crystallized.

repeatedly in 1 M NaCl adjusted to pH 3 with HCl, followed by water washings to increase pH to >5.5 and decrease conductivity to $<700\text{ }\mu\text{S/cm}$.

The AuCl_4^- solution was prepared from $\text{AuCl}_3\cdot\text{HCl}\cdot 4\text{H}_2\text{O}$ using deionized water giving Au concentrations of 10,000, 500 and 50 $\mu\text{g/L}$, respectively. The pH values were adjusted to 3, 4, 5, 6, 7, 8 and 9, respectively, using HCl and NaOH. The cleaned kaolinite (1 g) was added to 100 mL of AuCl_4^- solutions and subsequently stirred with a glass bar, and then the containers were sealed. In the Shewushan supergene gold deposit, the inclusion data have shown that the hydrothermal temperatures mainly ranged from 110 to 290°C, therefore, our adsorption experiments were carried out both at ambient temperature and at 120°C in a drying oven, which was modeled as the hydro-

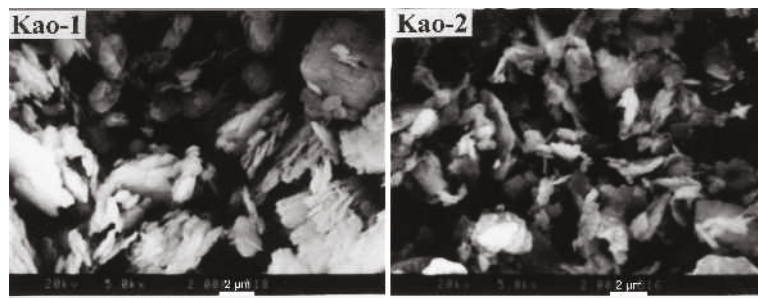


Figure 2. SEM images of the samples revealing the mineral composition of kaolinite and the larger particle size of kaolinite in Kao-1 compared with Kao-2.

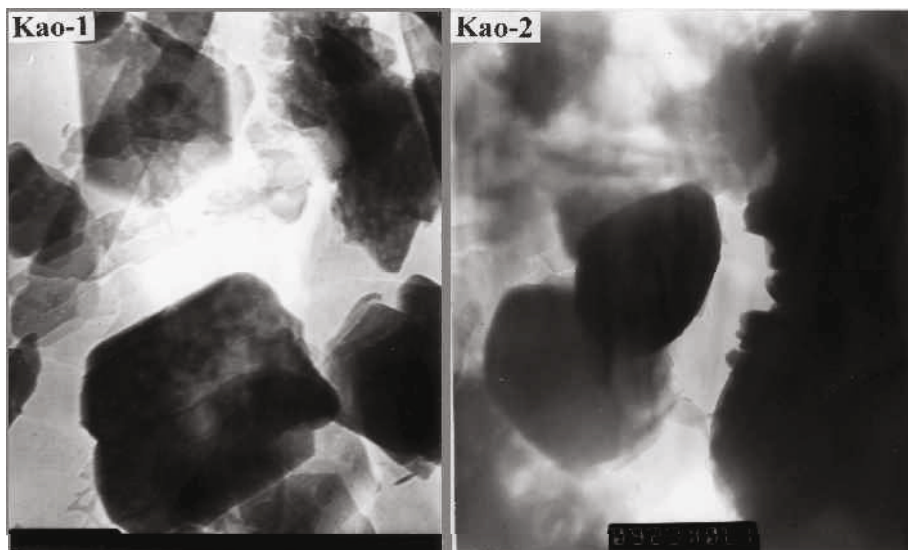


Figure 3. TEM images of kaolinites Kao-1 and Kao-2. Kao-1 particles have sharp hexagonal outlines and Kao-2 particles more rounded hexagonal outlines.

thermal solution. As shown by the previous experiments, in low-pH solutions, the AuCl_4^- complex was efficiently adsorbed onto kaolinite at three different Au concentrations and with different crystallinities; therefore, for the adsorption model investigation, the Au concentration of 4000 $\mu\text{g/L}$ was prepared with a pH value of 5, a different amount of the Kao-1 sample was used, and the reactions were performed at ambient temperature. The reacted kaolinite was separated from solution by filtration through 0.22 μm polycarbonate filters after a reaction time of 48 h, then the filtrate was analyzed for Au using an Hitachi Z-6000 polarized Zeeman flame atomic absorption spectrophotometer (FAA), or a Perkin-Elmer Zeeman/3000 graphite furnace atomic absorption spectrophotometer (GFAA). The detection limit for Au by FAA was 0.5 mg/L ; when Au concentrations measured by FAA were <0.5 mg/L , the GFAA was used. Three Au measurements were made for each sample. The detection limit for Au by GFAA is <1 $\mu\text{g/L}$. Taking into account uncertainties such as instrumental instability, the practical detection limit for trace Au is estimated to be 1 $\mu\text{g/L}$. The adsorption of AuCl_4^- complex by kaolinite was calculated from the change in Au concentration in the solution. The error in measurement did not exceed 5%.

Table 1. Particle-size distribution of the two samples of kaolinite.

Size (μm)	Kao-1	Kao-2
>10	8.39%	5.57%
10–5	29.77%	30.38%
5–2.5	51.15%	40.25%
<2.5	10.69%	23.80%
Average size	5.39 μm	4.98 μm

RESULTS

The XRD patterns of the two samples are shown in Figure 1. The results suggest that the Hinckley indexes (HI) for Kao-1 and Kao-2 kaolinites were 1.42 and 0.35, respectively. This indicates that sample Kao-1 is well crystallized and that Kao-2 is poorly crystallized.

The results of particle-size analysis of the two samples are given in Table 1, which shows that the particle sizes of both samples vary from mainly 2.5 to 10 μm . The portion of particle size <2.5 μm in sample Kao-2, however, is much larger than that in sample Kao-1, and the average particle sizes of the Kao-1 and Kao-2 samples are 5.39 and 4.98 μm , respectively. The chemical compositions of the samples listed in Table 2 suggest that both of the samples are composed mainly of SiO_2 , Al_2O_3 and H_2O^+ , in good agreement with the chemical composition of kaolinite. This reflects the high purity of the samples.

The results of the adsorption experiments in Table 3 show the amount of Au removed by the two samples of kaolinite at ambient temperature and 120°C, respectively. The effect of temperature, pH, and the crystallinity of kaolinite was determined. The amount of Au removed by the kaolinite samples was plotted as a function of pH, which showed that the adsorption of Au by the two kaolinites is similar. Figure 4 shows the amount of Au adsorbed by sample Kao-1 in 10,000 $\mu\text{g/L}$ solution with pHs from 3 to 9. As can be seen from Table 3 and Figure 4, the two samples of kaolinite adsorbed AuCl_4^- complex strongly over a wide range of pH values from 3 to 9 at both ambient temperature and 120°C. In lower-pH solutions, the AuCl_4^- complex was efficiently adsorbed onto kaolinite at three different Au concentrations and with different crystallinities; almost all the Au in solutions was adsorbed by kaolinite. However, the

Table 2. Chemical composition (wt.%) of the kaolinite samples.

	SiO ₂	Al ₂ O ₃	Fe ₂ O ₃	MgO	CaO	Na ₂ O	K ₂ O	MnO	TiO ₂	H ₂ O ⁺
Kao-1	44.35	39.81	0.50	0.53	0.14	1.16	0.87	0.015	0.57	12.19
Kao-2	47.16	37.84	0.61	0.11	0.03	1.75	0.78	0.002	0.09	11.63

amount of Au adsorbed decreased with increasing pH. At pH 5, which showed an obvious decreasing tendency, and particularly in the neutral solution at pH 7, the amount of adsorption was the lowest in the whole range of the curve. In alkaline solutions, the amount of adsorption increased gradually with increases in pH. The solution temperature played an important role in adsorption of the AuCl₄⁻ complex. The amount of adsorption was greater at 120°C than at ambient temperature at the same pH and for the same kaolinite sample. It was also found that the crystallinity of the kaolinite affected the adsorption of the AuCl₄⁻ complex. The lower the crystallinity of kaolinite, the greater the degree of adsorption. On the other hand, Au concentration had a significant effect on the adsorption of Au in the system. In a solution with high Au concentration, more of the Au was adsorbed by kaolinite, though the percentage of adsorption became lower relative to the system with low Au concentration, suggesting that the kaolinite sample was not able to scavenge the AuCl₄⁻ complex efficiently in the high AuCl₄⁻ concentration condition. Most of the Au was adsorbed by kaolinite, especially at low concentrations of Au, e.g. the 50 µg/L solution, when the adsorption was largely independent of the pH and crystallinity of kaolinite.

Table 4 shows the results of adsorption of AuCl₄⁻ by different masses of the Kao-1 sample at ambient temperature with the solution pH of 5. Adsorption isotherms were determined for the adsorption of AuCl₄⁻ complex by kaolinite.

DISCUSSION

Adsorption isotherms

Both the Langmuir and Freundlich equations have been used in this study to model the adsorption data shown in Table 4. The Langmuir equation is based on

there being a finite number of coordination sites on the surface of an adsorbent. The Freundlich equation is an empirical isotherm, which predicts unlimited adsorption.

The Langmuir equation is written as:

$$\frac{\Gamma}{\Gamma_\infty} = \frac{KC_j}{1 + KC_j} \quad (1)$$

where Γ is the adsorption density (mol kg⁻¹) and Γ_∞ corresponds to a saturated coordination site type or a monolayer coverage, C_j is the activity of the j species at the solid/solution interface, and K is a constant quantifying the affinity of the adsorbate for the adsorbent. K is related to the ratio of the fraction of molecules which collide with an empty adsorbent surface and adhere to it and the ratio of desorption of molecules from a saturated surface. Equation 1 is often transformed as follows:

$$\frac{1}{\Gamma} = \frac{1}{\Gamma_\infty KC_j} + \frac{1}{\Gamma_\infty} \quad (2)$$

where equation 2 describes a straight line. Γ_∞ and K were determined by plotting Γ^{-1} as a function of C_j^{-1} . When plotting the adsorption isotherm, Γ was expressed in g kg⁻¹ and C_j in mg L⁻¹. From the isotherm Γ_∞ is 4.25 g kg⁻¹, and K is 0.62, with an R^2 value of the Langmuir fit of 0.89.

In developing equation 1, Langmuir proposed that Γ_∞ was a finite number corresponding to a monolayer coverage. Exceeding Γ_∞ resulted in the formation of multiple layers of adsorbent. Obviously, the Γ_∞ value of 4.25 g kg⁻¹ obtained from the fit for kaolinite disagrees with the experimental value of 8.55 g kg⁻¹, and seems to be incompatible with monolayer coverage of the surface for the large specific area of kaolinite (Yuri *et al.*, 1998). It can be concluded therefore that Γ_∞ is equated with a group of equivalent adsorption sites which have the same likelihood of coordinating with the adsorbate; saturation of one group type may be achieved without forming a monolayer coverage. As shown in Table 4, the sharp increase in Γ at Au concentration C_j around 2.0 mg L⁻¹ is consistent with the presence of at least one other type of site on the surface.

The Freundlich equation is as follows:

$$\Gamma = kC_j^{1/n} \quad (3)$$

Taking ln of equation 3 and rearranging

$$\ln \Gamma = (1/n) \times (\ln C_j) + \ln k \quad (4)$$

Figure 4. Adsorption of Au from a 10,000 µg/L solution by the Kao-1 kaolinite at both ambient temperature and 120°C.

Table 3. Adsorption of AuCl_4^- by the two samples of kaolinite with different crystallinities at ambient temperature and 120°C.

pH	Initial Au	Kao-1		Adsorbed Au	Initial Au	Kao-2	
		Equilibrium Au	Adsorbed Au			Equilibrium Au	Adsorbed Au
Ambient							
3	50 $\mu\text{g/L}$	1±0.0 $\mu\text{g/L}$	4.9 mg/kg		50 $\mu\text{g/L}$	1±0.0 $\mu\text{g/L}$	4.9 mg/kg
4	50	1±0.0	4.9		50	1±0.1	4.9
5	50	1±0.1	4.9		50	2±0.0	4.8
6	50	1±0.0	4.9		50	3±0.1	4.7
7	50	17±0.6	3.3		50	11±0.3	3.9
8	50	3±0.2	4.7		50	4±0.2	4.6
9	50	2±0.1	4.8		50	3±0.1	4.7
3	500	2±0.0	49.8		500	1±0.1	49.9
4	500	4±0.1	49.6		500	2±0.0	49.8
5	500	6±0.3	49.4		500	7±0.2	49.3
6	500	5±0.1	49.5		500	10±0.3	49.0
7	500	29±1.3	47.1		500	36±1.4	46.4
8	500	20±0.8	48.0		500	25±0.7	47.5
9	500	16±0.7	48.4		500	19±0.7	48.1
3	10000	311±6.4	968.9		10000	23±0.4	997.7
4	10000	359±4.1	964.1		10000	23±0.3	997.7
5	10000	671±6.3	932.9		10000	384±14.2	961.6
6	10000	875±18.2	912.5		10000	2292±66.8	770.8
7	10000	3608±96.4	639.2		10000	3690±151.3	631.0
8	10000	3441±124.0	655.9		10000	3664±135.6	633.6
9	10000	3335±108.9	666.5		10000	3049±125.0	695.1
120°C							
3	50	1±0.1	4.9		50	1±0.0	4.9
4	50	1±0.0	4.9		50	2±0.1	4.8
5	50	1±0.1	4.9		50	3±0.1	4.7
6	50	3±0.1	4.7		50	4±0.2	4.6
7	50	8±0.3	4.2		50	4±0.1	4.6
8	50	8±0.2	4.2		50	4±0.1	4.6
9	50	2±0.0	4.8		50	3±0.2	4.7
3	500	1±0.1	49.9		500	2±0.1	49.8
4	500	1±0.0	49.9		500	1±0.0	49.9
5	500	1±0.1	49.9		500	1±0.0	49.9
6	500	42±1.8	45.8		500	10±0.3	49.0
7	500	45±2.0	45.5		500	11±0.4	48.9
8	500	39±1.3	46.1		500	8±0.3	49.2
9	500	18±0.9	48.2		500	8±0.1	49.2
3	10000	6±0.1	999.4		10000	12±0.2	999.8
4	10000	8±0.3	999.2		10000	25±0.7	997.5
5	10000	11±0.3	998.9		10000	41±1.0	995.9
6	10000	1720±69.1	828.0		10000	524±19.8	947.6
7	10000	3250±128.4	675.0		10000	3335±123.4	666.5
8	10000	3200±97.6	680.0		10000	3230±138.9	677.0
9	10000	2904±112.9	709.6		10000	2140±85.6	786.0

where Γ and C_j have the same meaning as in equation 1 and k and n are empirical constants, which were determined by plotting $\ln C_j$ vs. $\ln \Gamma$. Equation 4 describes a straight line where $1/n =$ slope and $\ln k =$ intercept. The values of n and k are 1.18 and 1.85, respectively, with an R^2 value of the Freundlich fit = 0.74. The Freundlich isotherm has two distinct linear regions, which has been claimed to indicate the existence of a heterogeneous surface (Benjamin and Leckie, 1981).

The isotherms obtained suggest that the adsorption data for the AuCl_4^- complex onto kaolinite will have both Langmuir shape and Freundlich shape. The surface of kaolinite is interpreted as having specific coordination sites with a high affinity for the AuCl_4^- complex. However, the poor fit of the equations is indicative of the existence of heterogeneous surfaces on kaolinite, and while both Freundlich and Langmuir adsorption isotherms model the data, the constants for the Langmuir

Table 4. Adsorption of AuCl_4^- by different masses of Kao-1 at pH 5 and ambient temperature.

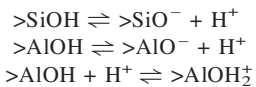
Mass of Kao-1 (g)	0.02	0.08	0.14	0.20	0.28	0.50	1.0
Equilibrium Au (mg/L)	2.290	1.973	1.596	1.195	0.997	0.424	0.106
Adsorbed Au (mg/g)	8.550	2.534	1.717	1.403	1.073	0.715	0.389

equation are perhaps more meaningful because they can be related to a physical model of the adsorption process.

pH dependence of adsorption

Table 3 and Figure 4 illustrate the amount of adsorption of AuCl_4^- complex at pH values between 3 and 9 which show that at pHs between 3 and 5 the amount of Au adsorbed was extremely large, which indicates that the AuCl_4^- complex was strongly adsorbed by kaolinite. However, the curve shows a rapid decrease between pH 5 and 7, and a steady increase between pH 7 and 9. This lack of complete adsorption at the various pH levels indicates that the available adsorption sites were saturated.

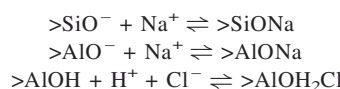
It is believed that (001) basal surfaces of kaolinite are positioning the oxygen anions that are either singly or doubly coordinated with underlying cations (Gerson, 1997), and edge surfaces are composed of exposed silica and alumina sheets (Williams and Williams, 1978). Edge sites dominate the complexation reactions of the surfaces, which are dominated by either siloxane sites in silica sheets or aluminol sites in gibbsite sheets (Sposito, 1984). The partially coordinated oxygen anions interact strongly with protons binding them and thus neutralizing the surface's inherently negative charge. Similar to quartz and silica surfaces (Bolt, 1957), the silanol sites on kaolinite are probably quite acidic, acting only as proton donors, whereas the aluminol sites are modeled as exhibiting amphoteric behavior. The proton-surface reactions can be described as:



where silanol sites are denoted by SiOH and aluminol by AlOH .

In low-proton activity solutions, the surfaces are typically negatively charged and many oxygen anions will lack bound protons. In high-proton activity solutions, singly protonated oxygen anions in aluminol sites will bind additional protons and the surfaces are positively charged. Therefore, at pH values <5 , the surfaces of kaolinite are positively charged and electrostatic attractive forces between AuCl_4^- and the positive surfaces of kaolinite in these increasingly acid solutions would further increase the likelihood of AuCl_4^- adsorption. At pH >5 , the surface of kaolinite would become negatively charged and repulsion of AuCl_4^- at the kaolinite/solution interface would be expected. This would tend to inhibit AuCl_4^- in the formation of a surface complex.

In electrolyte solution, as described by the triple-layer model (TLM) (Davis *et al.*, 1978; Hayes *et al.*, 1991), the solid surface is envisaged to be a charged surface to which adsorbing species are bound by chemical and electrostatic interactions, with charge-compensating counterions forming a diffuse layer of opposite charge in the overlying solution. Using the TLM model, Ward and Brady (1998) calculated speciation at the kaolinite/solution interface in 0.01 M NaCl at 25°C. The three surface reactions are:



Their results demonstrated that the silica sites remain neutral until pH >7 , at which point they begin to deprotonate significantly. At greater ionic strength and temperature, the Na complex $>\text{SiONa}$ becomes increasingly stable and the Na complex in alumina sites $>\text{AlONa}$ is increasingly generated. At pH values between 4 and 7, the alumina sites nearly completely deprotonate and $>\text{AlONa}$ becomes stable. In this scheme, the positively charged alumina sites will facilitate the AuCl_4^- adsorption at low pH. At pHs between 4 and 6, alumina sites will partially deprotonate and result in the decreased adsorption of AuCl_4^- . At pH near 7, alumina sites nearly completely deprotonate and adsorption reaches a minimum. On the other hand, at pH >7 adsorption increases significantly, mainly by the formation of a surface complex between the edge surfaces of kaolinite and AuCl_4^- . The adsorption properties of AuCl_4^- onto kaolinite reflects the surface chemistry of alumina sites, suggesting that adsorption reactions of the AuCl_4^- anion mainly occur at alumina sites.

Effect of temperature on adsorption

By comparing adsorption at the two temperatures, it can be clearly seen from Table 3 and Figure 4 that the solution temperature has a significant effect on the adsorption of the AuCl_4^- complex. In general, the percentage of adsorption of Au is greater at 120°C than at ambient temperature in the same pH solutions and for the same sample of kaolinite. However, the effect of temperature on adsorption varies with the Au concentration of the solutions and the crystallinity of the kaolinites. For the well crystallized kaolinite, as shown in Table 3 and Figure 4, at 120°C in solutions of pH <5 , the percentage of adsorption was $>98\%$. At pH 6 and 7, although the percentage of adsorption showed a decreasing tendency, the percentage of adsorption was the same

as that at ambient temperature in the same Au concentration solutions. In the solutions of pH >7, the percentage of adsorption increased sharply, whereas at ambient temperature the percentage of adsorption increased slowly. For the poorly crystallized kaolinite, the improvement of adsorption in 120°C solutions was much more obvious, especially for the solutions with Au concentrations of 500 µg/L and 50 µg/L, which demonstrated that at 120°C the percentage of adsorption was >92% in the 50 µg/L solution and >98% in the 500 µg/L solution over the pH range 3–9. As shown in Table 3 and Figure 4, the increase in temperature promoted the adsorption of AuCl_4^- for both samples of kaolinite, suggesting that an increase in temperature facilitated the formation of a surface complex at active sites on edge surfaces. However, the effect of temperature on adsorption was much more prominent in low-concentration solutions (50 µg/L, 500 µg/L) than that in a high-concentration solution (10,000 µg/L) at pH ≥5. The relative insensitivity to temperature in high-concentration solutions probably showed that in this condition the ion strength of the solution dominated the adsorption reaction on the edge surfaces. Chang and Sposito (1994) performed a computer simulation of the electrostatic interaction between the charged surfaces of clay mineral particles and electrolyte solution based on the Modified Gony-Chapman theory. Their results suggested that the positively charged edge surface affects clay-electrolyte interactions most significantly at low electrolyte concentration; a particle with a large enough edge surface (thickness >4.9 nm) may exhibit net anion exclusion at high electrolyte concentrations and net anion adsorption at low electrolyte concentrations.

Effect of crystallinity of kaolinite

Table 3 and Figure 4 show that the two samples of kaolinite with different crystallinity have similar adsorption properties. However, there are some variations between the two samples. In general, the amount of adsorption of the Kao-2 sample is larger than that of the Kao-1 sample at the same pH and AuCl_4^- concentration solution. The poorly crystallized sample (Kao-2) has greater capacity to scavenge the AuCl_4^- complex than the well crystallized sample (Kao-1) at pH 5–9, indicating more active sites in Kao-2 kaolinite than in Kao-1 kaolinite. In the poorly crystallized kaolinite sample, the crystals commonly developed terraces, steps and other rough surfaces, *e.g.* microvalleys and microhills on the crystal surfaces (Zbik and Smart, 1998), and the particles are smaller and thinner than the well crystallized kaolinite. Therefore, the poorly crystallized kaolinite shows larger specific area than the well crystallized kaolinite. In particular, the poorly crystallized kaolinite develops much more ragged and irregular edges and produces more active sites, which will in turn facilitate the adsorption process. Cases *et al.* (1986) investigated the surface properties of kaolinite with varying crystal-

larity. They pointed out that the decrease in the crystallinity of kaolinites is accompanied by an increase in the specific surface areas and particularly in the lateral surface areas, which contain active sites. They dominate the adsorption/desorption reactions because of the presence of >SiOH or >AlOH on the surfaces and there is an increase in the surface area from 2.47 m²/g for the well crystallized kaolinite with a Hinckley Index (HI) of 1.41, to 10.35 m²/g for the poorly crystallized kaolinite with HI 0.32. This suggests that the difference in crystallinity of the kaolinites will result in differences in the active sites and therefore will affect the adsorption reaction. In comparison with the two kaolinite samples, it can be found from Table 3 and Figure 4 that the sharp decrease in amount of adsorption at pH 5 is for the well crystallized kaolinite and at pH 6 is for the poorly crystallized kaolinite. This discrepancy is probably dominated by the characteristic surface charge properties of kaolinite. It is well known that kaolinite has heterogeneous surface charge. The basal surface of kaolinite is believed to carry a constant structural charge which is attributed either directly to the isomorphous substitution of Si^{4+} by Al^{3+} in the tetrahedral sheet of the mineral (van Olphen, 1951; Schofield and Samson, 1954; Flegmann *et al.*, 1969; Rand and Melton, 1977), or indirectly to the isomorphic substitutions in 2:1 layer-type clay mineral inclusions (Lim *et al.*, 1980; Jepson, 1984; Kim *et al.*, 1996). The charge on the edges is due to the protonation/deprotonation of surface hydroxyl groups and therefore depends on the solution pH. However, the density of constant structural charge (δ_0) and that of pH-dependent charge (δ_H) vary with the degree of crystallinity of kaolinites. The sign of δ_0 is always negative for kaolinite and the sign of δ_H varies with aqueous solution pH, taking on a zero value at the point of zero net proton charge and becoming negative at higher pH values (Sposito, 1992). Schroth and Sposito (1997) studied the charge property of kaolinites of varying crystallinity. Their results suggested that the equilibrium points of zero net proton charge values were ~5.0 for the well crystallized kaolinite and 5.4 for the poorly crystallized kaolinite, respectively. Thus, the difference in surface proton charge created by proton adsorption and desorption reactions will cause the variation in the surface charge property (protonation/deprotonation) at the same pH condition, and hence the solution pH values of the strongest adsorption of AuCl_4^- are <5 for the well crystallized kaolinite and <6 for the poorly crystallized kaolinite, respectively.

CONCLUSIONS

One of the primary observations from this study is that kaolinite can adsorb Au extremely effectively within the range of chemical parameters characteristic of a hydrothermal environment. Both the Langmuir and the Freundlich equation fits show the existence of hetero-

geneous surfaces on kaolinite. At pH 5 and ambient temperature, the adsorption density of kaolinite for Au(III) was up to 8.55 g kg^{-1} .

The adsorption of AuCl_4^- by kaolinite was dominated by the pH of the solutions. The percentage of adsorption varied from ~100% in acid solutions (pH < 5) down to ~64% and 68% in neutral to alkaline solutions at ambient temperature and 120°C, respectively, indicating that the adsorption of AuCl_4^- by kaolinite is pH dependent and involves surface complexation, mainly depending on the alumina sites on the edge surfaces of kaolinite crystals.

The percentage of adsorption was greater at 120°C than at ambient temperature in the same pH solutions and for the same sample of kaolinite. An increase in temperature promotes the adsorption of AuCl_4^- by kaolinite.

The two samples of kaolinite with varying crystallinity have similar adsorption properties. However, the poorly crystallized sample (Kao-2) had greater capacity to adsorb the AuCl_4^- complex than the well crystallized sample (Kao-1) at pH 5–9, indicative of a greater number of active sites in Kao-2 kaolinite than that in Kao-1 kaolinite. In addition, the adsorption decreased rapidly at pH 5 for the well crystallized kaolinite and pH 6 for the poorly crystallized kaolinite, possibly reflecting the difference in equilibrium points of zero net proton charge values for kaolinites of different crystallinity.

ACKNOWLEDGMENTS

This work was supported by the Natural Science Foundation of China (NSFC), allotment grant number 40172017. The authors wish to thank Dr Mu Shanbin for the SEM work, Dr Song Jinghong for the particle-size determination, and Prof. K.D. Stephen for improving the English. The authors are particularly grateful to Dr D.C. Bain, Dr W.F. Jaynes, Dr R.L. Frost and Dr A. Ruiz-Conde for their constructive comments and suggestions.

REFERENCES

- Benjamin, M.M. and Leckie, J.O. (1981) Multiple-site adsorption of Cd, Cu, Zn, and Pb on amorphous iron oxyhydroxide. *Journal of Colloid and Interface Science*, **79**, 209–221.
- Bolt, G. (1957) Determination of the charge density of silica sols. *Journal of Physical Chemistry*, **61**, 1166–1170.
- Boyle, R.W. (1979) The geochemistry of gold and its deposits. *Geological Survey of Canada Bulletin*, **280**.
- Cases, J.M., Cunin, P., Grillet, Y., Poinsignon, C. and Yvon, J. (1986) Methods of analysing morphology of kaolinites: relations between crystallographic and morphological properties. *Clay Minerals*, **21**, 55–68.
- Chang, F.C. and Sposito, G. (1994) The electrical double layer of a disk-shaped clay mineral particle: Effect of particle size. *Journal of Colloid and Interface Science*, **163**, 19–27.
- Davis, J.A., James, R.O. and Leckie, J.O. (1978) Surface ionization and complexation at the oxide-water interface. 1. Computation of electrical double layer properties in simple electrolytes. *Journal of Colloid and Interface Science*, **63**, 480–499.
- Flegmann, A.W., Goodwin, J.W. and Ottewill, R.H. (1969) Rheological studies on kaolinite suspensions. *Proceedings of the British Ceramics Society*, **13**, 31–45.
- Foster, R.L. (1970) Gold deposits at Slate Creek, northern Nye County, Nevada. *Economic Geology*, **66**, 965–966.
- Gerson, A.R. (1997) The surface modification of kaolinite using water vapour plasma, Pp. 227–235 in: *Computational Chemistry and Chemical Engineering* (G. Cisneros, J.A. Cogordan, C.M. Wang and M. Castro, editors). World Scientific Publishing Company Incorporation, River Edge, New Jersey, USA.
- Hayes, K.F., Redden, G.W. and Leckie, J.O. (1991) Surface complexation models: An evaluation of model parameter estimation using FITEQL and oxide mineral titration data. *Journal of Colloid and Interface Science*, **142**, 448–469.
- Hong, H. and Ye, X. (1998) Study on characteristics of the gold in the lateritic gold mine. *Journal of Chinese Electron Microscopy Society*, **17**, 267–271 (in Chinese).
- Hong, H., Wang, Q., Chang, J., Liu, S. and Hu, R. (1999) Occurrence and distribution of invisible gold in the Shewushan supergene gold deposit China. *The Canadian Mineralogist*, **38**, 1525–1531.
- Hyland, M.M. and Bancroft, G.M. (1989) An XPS study of gold deposition at low temperatures on sulphide minerals: reducing agents. *Geochimica et Cosmochimica Acta*, **53**, 367–372.
- Jepson, W.B. (1984) Kaolins: Their properties and uses. *Philosophical Transactions of the Royal Society of London*, **A311**, 411–432.
- Kim, Y., Cygan, R.T. and Kirkpatrick, R.J. (1996) ^{133}Cs NMR and XPS investigation of cesium adsorbed on clay minerals and related phases. *Geochimica et Cosmochimica Acta*, **60**, 1041–1052.
- Lim, C.H., Jackson, M.L., Koons, R.D. and Helmke, P.A. (1980) Kaolinites: Sources of differences in cation-exchange capacities and cesium retention. *Clays and Clay Minerals*, **28**, 223–229.
- Mycroft, J.R., Bancroft, G.M., McIntyre, N.S. and Lorimer, J.W. (1995) Spontaneous deposition of gold on pyrite from solutions containing Au(III) and Au(I) chlorides. Part: A surface study. *Geochimica et Cosmochimica Acta*, **59**, 3351–3365.
- Ogryzlo, S.P. (1935) Hydrothermal experiments with gold. *Economic Geology*, **30**, 400–424.
- Rand, B. and Melton, I.E. (1977) Particle interactions in aqueous kaolinite suspensions, I. Effect of pH and electrolyte upon the mode of particle interaction in homoionic sodium kaolinite suspensions. *Journal of Colloid and Interface Science*, **60**, 308–320.
- Renders, P.J.N. and Seward, T.M. (1989) The stability of hydro-sulphido- and sulphido-complexes of Au(I) and Ag(I) at 25°C. *Geochimica et Cosmochimica Acta*, **53**, 245–253.
- Rosliyakov, H.A. (1990) Occurrence of Au in soil and its indicative significance. *Science and Technology of Gold Geology*, **23**, 32–37 (translated from Chinese).
- Schofield, R.K. and Samson, H.R. (1954) Flocculation of kaolinite due to the attraction of oppositely charged crystal faces. *Discussions of the Faraday Society*, **18**, 135–145.
- Schroth, B.K. and Sposito, G. (1997) Surface charge properties of kaolinite. *Clays and Clay Minerals*, **45**, 85–91.
- Seward, T.M. (1973) Thio complexes of gold and the transport of gold in hydrothermal ore solutions. *Geochimica et Cosmochimica Acta*, **37**, 379–399.
- Seward, T.M. (1984) The transport and deposition of gold in hydrothermal systems, Pp. 165–181 in: *Gold'82: The Geology, Geochemistry and Genesis of Gold Deposits* (R.P. Foster, editor). A. A. Balkema Press, Rotterdam, Netherlands.
- Sposito, G. (1984) *The Surface Chemistry of Soils*. Oxford

- University Press, New York, 234 pp.
- Sposito, G. (1992) Characterization of particle surface charge. Pp. 291–314 in: *Environmental Particles* (J. Buffel and H. van Leeuwen, editors). Lewis Publisher, Chelsea, Michigan, USA.
- Sutheimer, S.H., Maurice, P.A. and Zhou, Q. (1999) Dissolution of well and poorly crystallized kaolinites: Al speciation and effects of surface characteristics. *American Mineralogist*, **84**, 620–628.
- van Olphen, H. (1951) Rheological phenomena of clays sols in connection with the charge distribution on the micelles. *Discussions of the Faraday Society*, **11**, 82–84.
- Ward, D.B. and Brady, P.V. (1998) Effect of Al and organic acids on the surface chemistry of kaolinite. *Clays and Clay Minerals*, **46**, 453–465.
- Williams, D.J.A. and Williams, K.P. (1978) Electrophoresis and zeta potential of kaolinite. *Journal of Colloid and Interface Science*, **65**, 79–87.
- Ye, X., Wang, G., Sun, S., Liu, Y., Zhou, L., Liu, S., Xue, D., Rivers, L. and Jones, K. W. (1994) Microscopy study on submicrometer gold in a Carlin-type gold deposit, Southwestern Guizhou, China. *Science in China*, **D24**, 883–889 (in Chinese).
- Yuri, B., Mietek, J. and Patricia, M. (1998) Adsorption characterization of two clay minerals society standard kaolinites. *Journal of Colloid and Interface Science*, **205**, 528–530.
- Zibk, M. and Smart, R.St.C. (1998) Nanomorphology of kaolinites: comparative SEM and AFM studies. *Clays and Clay Minerals*, **46**, 153–160.

(Received 11 February 2002; revised 6 June 2003; Ms. 633; A.E. William F. Jaynes)